258495   **GM**   NHTSA-98-3585

General Motors Corporation
Legal Staff

Facsimile   Telephone
(586) 492-2928   (586) 947-9212

DEC 2 0 2002

Annette M. Sandberg,   DHTSA-98-3585-585
Deputy Administrator
NATIONAL HIGHWAY TRAFFIC
  SAFETY ADMINISTRATION
400 Seventh Street, S.W., Room 5220
Washington, DC 20590

Dear Ms. Sandberg:

Re: **Settlement Agreement**
       Section B. Fire Safety Research

Enclosed is a publication prepared by Robert L. McMasters IV and Indrek S. Wichman of
Michigan State University, entitled, "Compound Material Thermal Parameters for a Layered
Material Resembling an Automobile Firewall." It relates to Project B.15 (Theoretical and
Experimental Study of Thermal Barriers Separating Automobile Engine and Passenger
Compartments).

This publication appeared in the July-August 2002 issue of *Heat Transfer Engineering* (Volume
23, Number 4). Note that GM was not made aware of this publication until after it was
published.

Yours truly,

D. K. Nowak-Vanderhoef

Deborah K. Nowak-Vanderhoef
Attorney

Enclosure

heat transfer engineering

heat transfer engineering

Compound Material Thermal Parameters for a Layered Material Resembling an Automobile Firewall

ROBERT L. McMASTERS IV and INDREK S. WICHMAN

Department of Mechanical Engineering, Michigan State University, East Lansing, Michigan, USA

Heat transmission through a layered compound material consisting of carbon steel backing and insulation (either aluminized silver or fiberglass) was examined to determine thermal properties. The heat flux impinged on the insulation material side of this simulated "firewall." A heat transfer model was developed that could, in principle, be used to predict the heat transfer through layered compound materials using techniques of thermal property parameter estimation. The parameter estimates are based on thermocouple measurements of surface temperatures during heating on both sides of the material. The experiment analyzed in this article involved a vertical plate exposed on the insulation side to a transient step-applied radiant heat flux. The transient temperature measurements were fitted to heat transfer models. Thermal diffusivity and Biot number were estimated using ordinary least-squares nonlinear regression.

The purpose of this research is to examine heat transfer through a layered compound material that resembles an automobile "firewall" under conditions similar to those encountered when the insulation side of the assembly is subjected to fire-level heat fluxes. This research was part of a five-year project on vehicle fires undertaken by General Motors under a settlement agreement between the U.S. Department of Transportation and General Motors Corporations, dated March 7, 1995. Fire simulation tests were performed in which the layered material was heated by a radiant panel on the insulation side while temperature measurements were being made on both sides (see Figure 1). The radiant fluxes applied to the insulation surface were comparable to fluxes experienced in a fire, but at no time during the experiment was fire actually present.

In the tests, techniques commonly employed in standardized property analysis tests were not enforced. These include thermal isolation of the tested samples, suppression of convective flow, and minimization of macroscopic radiation interactions with other surfaces. The air in the test chamber flowed across the insulated (heated) side and steel rear, and the radiant flux emitted from the rear surface entered the ambient surroundings. The only controlled radiant flux on the front (insulation) surface occurred between heater and insulation. On both sides, heat conduction and convection to the ambient were uncontrolled.

Address correspondence to Dr. Robert L. McMasters IV, Department of Mechanical Engineering, Michigan State University, East Lansing, MI 48824-1226, USA. E-mail: mcmaste7@msu.edu
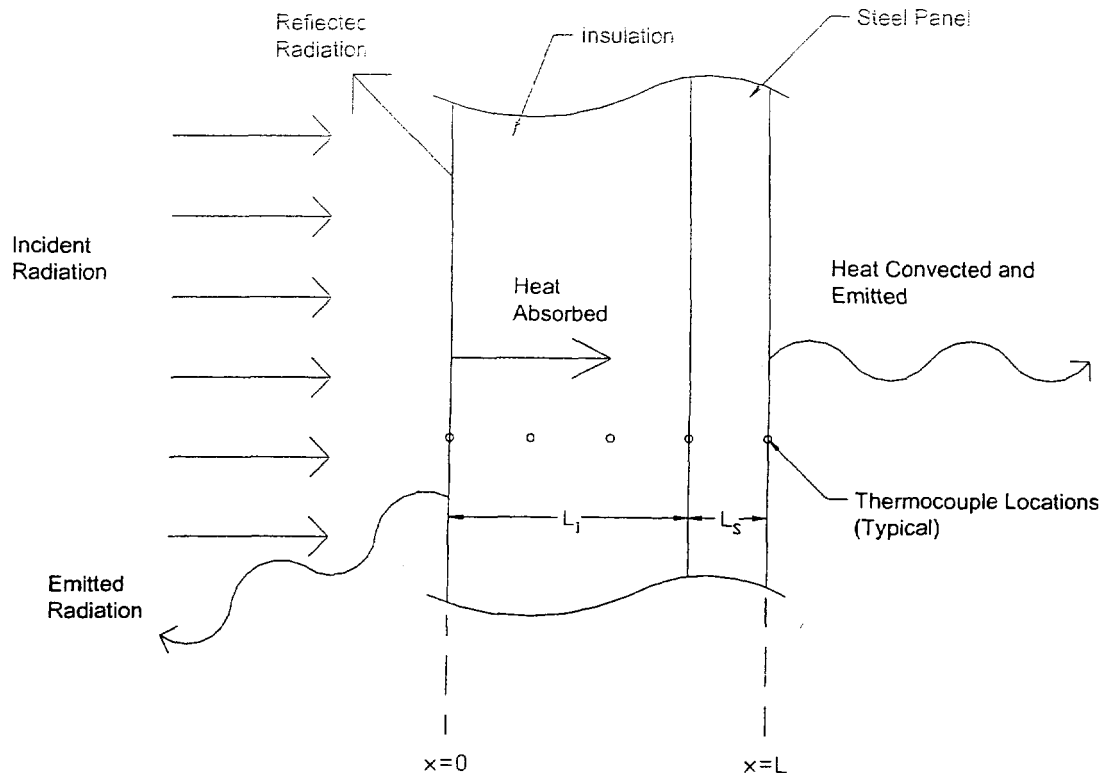
Figure 1 Schematic diagram of the one-dimensional two-layer material. The insulation is heated by the radiant flux from the left. Note the position of the thermocouples (TC). Also note that $L = L_S + L_I$ is the thickness of the compound material. Location $x = 0$ is the heated face, while location $x = L$ is the rear surface.

Because these various heat losses are difficult to include accurately in a model, this research focuses on the development of a "lumped" model of the two-layer assembly across which the heat transfer occurs. The temperature is monitored by static (fixed-point) thermocouple measurements on both sides of the material layer. The "lumped" model consists of the energy equation, initial condition, temperature boundary condition on the heated side, heat loss condition on the rear side, and temperature boundary condition on the rear side. This overdetermined system enforces conformity to the measured surface temperatures by fixing two parameters: (1) assembly thermal diffusivity and (2) heat loss coefficient from the rear surface.

The practical aim of this research is to determine how much of the incident power (measured from the input heat source) can be transmitted to the rear side of the firewall and to estimate thermal parameters in this extreme environment. This analysis employs the practice of "applied engineering parameter estimation."

This research has three goals. One is to estimate material parameters for calculating heat transfer through layered materials. The methods of parameter estimation [1] are used with the measurements in order to determine the model thermophysical parameters. The parameters are fixed upon choice of the model to describe the experiment. They are determined by fitting the model to the measurements. Models of varying de-

grees of complexity are possible. The second research goal is to determine the extent to which the layered material can be considered as a "compound" material with respect to its thermal properties and rates of heat transfer. The model to which the data are fitted should be simple enough to be amenable to engineering analysis. The third research goal is to determine, if possible, why compound materials consisting of layers of materials whose individual properties are known do not necessarily produce accurate estimates of heat transfer rates. In a companion study, the thermal properties for individual insulations were estimated [2, 3]. These estimations proved to be difficult and were carried out in a 50°C temperature range between 300 and 350°C, which is much narrower than the range examined here.

Recent estimations of thermal diffusivity include experiments performed on diamond films [4]. The techniques used in [4] for high-conductivity materials, however, do not lend themselves well to the experiments examined in this article. Reference [5] describes mathematical methods, which may be employed in thermal diffusivity measurements. Methods of nonlinear least-squares minimization are described in [1]. The heat sources and sinks described in [5] provide a novel way to control heat flux in a thermal diffusivity measurement. In this research, the heat loss occurs by convection, conduction, and radiation to the ambient surroundings. The multilayered material tested in [6] is similar to the

multilayer material tested in the present research. In [6] the multilayer material was heated by a laser flash, not a continuous (and time-varying) incident radiant flux as was used here. In summary, thermal parameter estimations employ a more meticulously controlled experimental setup that does not typically resemble a real application. These tests, however, were meant to examine the nature of heat transfer across the material, not its thermal properties.

1. EXPERIMENT

The tests employed a 32 × 32 cm heating panel to radiantly heat a layer of insulation attached to a flat steel panel 1/32 in. (~0.8 mm) thick (see Figure 1). The insulation faces the "fire side" of the "firewall" assembly. Three type K thermocouples (TCs) were intrinsically welded to both sides of the steel panel and three TCs were located in the insulation as shown in Figure 1. There was no formal attachment of the thermocouples to the insulation material; the thermocouples were embedded into the insulation materials and were supported by the material fibers themselves. The TCs were all unshielded. The thermocouples that were used to measure the temperature of the metal plate were 24 gauge and were intrinsically welded to the surfaces of the plate. The thermocouples that were used to measure temperature in the insulating media were 30 gauge with a bead size of approximately $\frac{1}{2}$ mm. The standard deviation of the noise in any of the TCs ranged from 1.3 to 2.2°C. The experimental procedure involved continuous heating for the duration of the test.

Seven experiments were conducted, designated here as test 1–7. Test 1 resulted in the detachment of the insulation layer from the steel panel and was discarded from this analysis. Tests 2–4 used a fiberglass insulation of 1.9 cm thickness. Tests 5–7 used a reflective aluminized silica insulation of 0.16 cm thickness. Both insulations were fibrous. The degree of contact between the TCs and the insulation was not rigorously evaluated

and may have varied between tests (and possibly during each test) because of material change during heating, such as shrinkage and thermal alteration of fibers. Although certain individual TCs were located under the incident surface of the insulation layer, the temperatures they measured were not necessarily an accurate indication of the actual insulation surface temperature. Experiments were conducted at separation distances (between heating panel and steel panel) ranging from 9 to 12 cm. The heater was utilized at three intensities, 25%, 50%, and 100% of the 15-kW maximum power. Table 1 shows the radiant intensities for each test. These intensities are representative of "firelike" conditions, with values between 10 and 100 kW/m^2. Separate tests of the radiant panel using heat flux gauges indicated that the radiant heat flux varied less than 5% over an area of approximately 10 cm × 10 cm at the center of the panel. As shown in Figure 1, the panel directly faced the heater. Both panel and heater were vertical. Temperature and heat flux measurements were recorded at 1-s intervals during each experiment. Heat flux data were not used in this analysis.

The challenging, and unresolved, problem of quantifying the contact resistance between two different materials can produce large disparities between predicted and actual behavior [7]. However, contact resistance is often negligible when considering insulation material, and at worst, does not have a large effect. In addition, it is very difficult to estimate thermal properties for fibrous materials accurately, because of the problems of locating TCs, of proper packing density, and for many reasons described in publications such as [2, 3, 8]. Finally, insulations are sometimes lined externally with a polymeric material added for ease of handling, referred to as a "scrim" [9]. As an added complication, the "scrim" can, for high radiant fluxes, burn off the face of the insulation, exposing the insulation beneath directly to the radiant flux. One is left with the somewhat inaccurate (but robust) option, if engineering results are sought, of modeling the material layer as a single compound material, regardless of one's intuitive understanding that

Table 1 Estimated parameters (Direct Model 1)

Material	Test	Diffusivity (cm²/s)	Biot number (unitless)	Residual std. dev. (°C)	Temperature rise ΔT (°C)	Average incident intensity for 0–5 min (kW/m²)
Fiberglass, 1.96 cm thick	2	0.00939	2.649	2.568	171	43.5
	3	0.00894	0.359	8.590	336	64.3
	4	0.00521	6.182	2.107	66	14.5
Aluminized silica, 0.16 cm thick	5	0.000705	1.307	2.265	68	38.6
	6	0.000202	1.527	2.359	26	14.1
	7	0.000824	1.331	2.741	156	67.1

This table shows each test number with estimated diffusivity, Biot number, and residual standard deviation. The quantities ΔT and incident intensity are experimental parameters. Note that their magnitudes follow idealized trends.

such an approach is scientifically invalid. The thermo-physical properties of the "scrim" are generally different than those of the insulation it protects.

2. COMPOUND MATERIAL MODELS

In order to estimate the heat transfer through the compound material, a model for heat conduction through the material is needed. Precise mathematical models for compound materials are quite complicated and are difficult to solve even numerically; see [8]. All real materials have temperature-dependent thermophysical properties. In addition, fibrous insulating materials may allow radiation to penetrate the irradiated surface before being fully absorbed. Contact conductance between imperfectly joined materials can be estimated only empirically. It is postulated here that the "scrim" absorbs the incident radiant flux at the surface and that no radiation penetrates the surface. In Section 2.2 another model is examined in which insulation and steel layers are considered separately.

The models used here are based on the equation for conservation of energy in the material. In general,

$$\rho c \frac{\partial T}{\partial t} = \frac{\partial}{\partial x}\left(k \frac{\partial T}{\partial x}\right) \tag{1}$$

In the derivation of Eq. (1), the conductive flux $k \partial T/\partial x$ and its first derivative must be continuous functions of position. Constancy of ρc is not required.

The approach used here will be to formulate two separate models which are "fitted" to the experimental data in the hope that they will indicate the most useful means for modeling such compound materials. This work illustrates the difficulty associated with making heat transfer estimates in practical engineering situations. The compound properties derived are produced by a combination of the separate materials, the contact resistance, the material property changes, and the various heat exchanges at the boundaries. The formulation of a second separate model is intended to demonstrate the attempts made toward accounting for inadequacies in the first model. Despite the simplicity of the first model (Model 1), it will be seen that it is more robust and generally the most dependable model of those applied to the data.

2.1. Direct Model 1: Homogeneous Compound Material

Constant k is assumed and constant α with respect to t, x, and T. It is apparent from this analysis that

these approximations are not valid. Nevertheless, the constant-property model provides a rational basis for estimating compound material properties. Equation (1) becomes

$$\rho c \frac{\partial T}{\partial t} = k \frac{\partial^2 T}{\partial x^2} \tag{2}$$

subject to the boundary conditions

$$T(0, t) = T(t) \tag{3}$$

$$-\left(k \frac{\partial T}{\partial x}\right)_{L,t} = h[T(L, t) - T_\infty] \tag{4}$$

and the initial condition $T(x, 0) = T_\infty$. Dividing Eq. (2) by k and Eq. (4) by k/L yields the parameter groups α and Bi. In the definition of Bi, $L = L_I + L_S$ is the width of the compound material.

Since the thermophysical parameters contained in α and Bi do not appear individually in the mathematical model, parameter estimates for k, ρ, c, h cannot be made independently. If, for example, the conductive heat flux at the front surface of the insulation were known, the boundary condition could be written as $-(k \partial T/\partial x)_{x=0} = q(0, t)$. In this case the k value of the compound material could then be estimated as a separate parameter. Here the surface heat transfer at the front boundary includes incident and emitted radiation, natural-convection losses, and conduction into the insulation. It was not possible to isolate the conductive flux, therefore only α and Bi were estimated.

The solution of Eqs. (2)–(4) is found using a finite-difference method described in [10]. The solutions were verified with a conductive heat transfer program developed independently by Professor A. Haji-Sheikh of the University of Texas at Arlington [11].

2.2. Direct Model 2: Separate Panel and Insulation

In model 2 the thermal properties of the insulation layer are assumed constant. The thermal properties of the steel layer, considered known, are $k_S = 49.2$ W/m K, $(\rho c)_S = 3.93 \times 10^6$ J/kg m^3 K, [12], so that $\alpha_S = 0.124$ cm^2/s. The initial condition is given as in Section 2.1. The temperature distribution on the heated surface is given by Eq. (3), while the boundary condition at the back surface is given by Eq. (4).

Now a description is given for the two boundary conditions at the interface of the insulation and steel. The first condition is continuity of temperature. The second

condition arises by writing Eq. (1) as $\rho c \, \partial T / \partial t = -\partial q / \partial x$ with $q = -k \, \partial T / \partial x$ and then discretizing to find

$$\left[\frac{(\rho c)_I \Delta x_I + (\rho c)_S \Delta x_S}{2 \Delta t} \right] T_i^{j-1} = -\frac{k_I}{\Delta x_I} T_{i-1}^j$$

$$+ \left[\frac{k_I}{\Delta x_I} + \frac{k_S}{\Delta x_S} + \frac{(\rho c)_I \Delta x_I + (\rho c)_S \Delta x_S}{2 \Delta t} \right] T_i^j$$

$$- \frac{k_S}{\Delta x_S} T_{i+1}^j \tag{5}$$

where separate step sizes (Δx_I and Δx_S) are used on the two sides of the interface. In the process of parameter estimation separate α values are employed in each material. In the case $\Delta x_I = \Delta x_S = \Delta x$ when α_I and α_S are *fixed* and k_I and k_S are *specified*, the resulting ρc values are also *fixed*. The preceding Eq. (5) contains only the ratios α_S / α_I and $(\rho c)_S / (\rho c)_I$. Individual values of k and ρc in each material cannot be evaluated separately. Consequently, this parameter estimation technique evaluates only α_I and α_S and Bi at the back surface. At the back surface the boundary condition is written in discretized form as

$$(\rho c)_S \Delta x_S / \Delta t \left(T_n^j - T_n^{j-1} \right)$$

$$= \left(T_{n-1}^j - T_n^j \right) k_S / \Delta x_S + h \left(T_\infty^j - T_n^j \right) \tag{6}$$

which can be rearranged to give

$$-T_{n-1}^j + \left(1 + \frac{\Delta x^2}{\alpha_S \Delta t} + \frac{h \Delta x}{k_S} \right) T_n^j$$

$$= \frac{\Delta x^2}{\alpha_S \Delta t} T_n^{j-1} + \frac{h \Delta x}{k_S} T_\infty \tag{7}$$

showing that only α_S and Bi $= h \Delta x / k_S$ can be estimated. The parameter Bi is defined with respect to the properties of the steel.

3. PARAMETER ESTIMATION

The parameters α and Bi can be estimated by comparing the measured temperatures to the computed temperatures at the near face $x = L = L_I + L_S$ (see Figure 1). Parameters α and Bi are determined by minimizing the sum of squares of the difference between computed and measured temperatures. The expression to be minimized through an iterative nonlinear regres-

sion procedure [1] is

$$S = \sum_{i=1}^{N} (Y_i - T_i)^2 \tag{8}$$

In order to refine parameter estimates between successive iterations it is necessary to compute the sensitivity coefficients. These are obtained by differentiating the solution for the T with respect to α and Bi. Since the solution is obtained numerically, the derivatives are approximated from the solution using a finite difference approximation. Figure 2 shows "modified" sensitivity coefficients, which are derivatives multiplied by the applicable parameter, i.e., $X_n = p_n \partial T / \partial p_n$, where X_n is the modified sensitivity coefficient and p_n is the parameter. Magnitudes of the X_n can be compared directly because they all have units of temperature. Since the solution for this particular analysis is computed numerically through finite differences, the sensitivity coefficients are necessarily computed in this way as well.

3.1. Direct Model 1

The estimated parameters are shown in Table 1. There is variation in the estimated α between experiments with the same material. This may be due to the variations in heating caused by changes in the insulation in the separate tests under different heat fluxes. Physical changes in the insulation may alter the corresponding thermal response for the separate experiments in Table 1. Variation in the contact resistance may also cause the differing values. The high temperatures may cause the material to sag, deform, and erode during the experiment. These behaviors of the materials under heating can generate experimental variations.

There is a variation with temperature rise of the property α from the data in Table 1. Between tests 2 and 4, the value of α increases from 5.2×10^{-3} cm^2/s for a ΔT of 66°C to 9.0×10^{-3} cm^2/s for a ΔT ranging from 171 to 336°C (tests 2 and 3). A similar rise of α with respect to ΔT is found in tests 5–7, with $\alpha = 2 \times 10^{-4}$ cm^2/s when $\Delta T = 26$°C (test 6) up to $\alpha = 8 \times 10^{-4}$ cm^2/s when $\Delta T = 156$°C. In both cases, most of the variation appears when ΔT is in the vicinity of 50°C. Beyond $\Delta T \approx O(100$°C$)$, relatively little α variation is observed (compare tests 2 and 3 and tests 5 and 7). The value of Bi varies throughout each series of tests. For the tests with fiberglass, with approximately 10 times larger α, the variation of Bi is more pronounced as a greater relative amount of front-surface thermal energy reaches the back surface. For the aluminized silica, whose compound α is approximately 10 times smaller than that
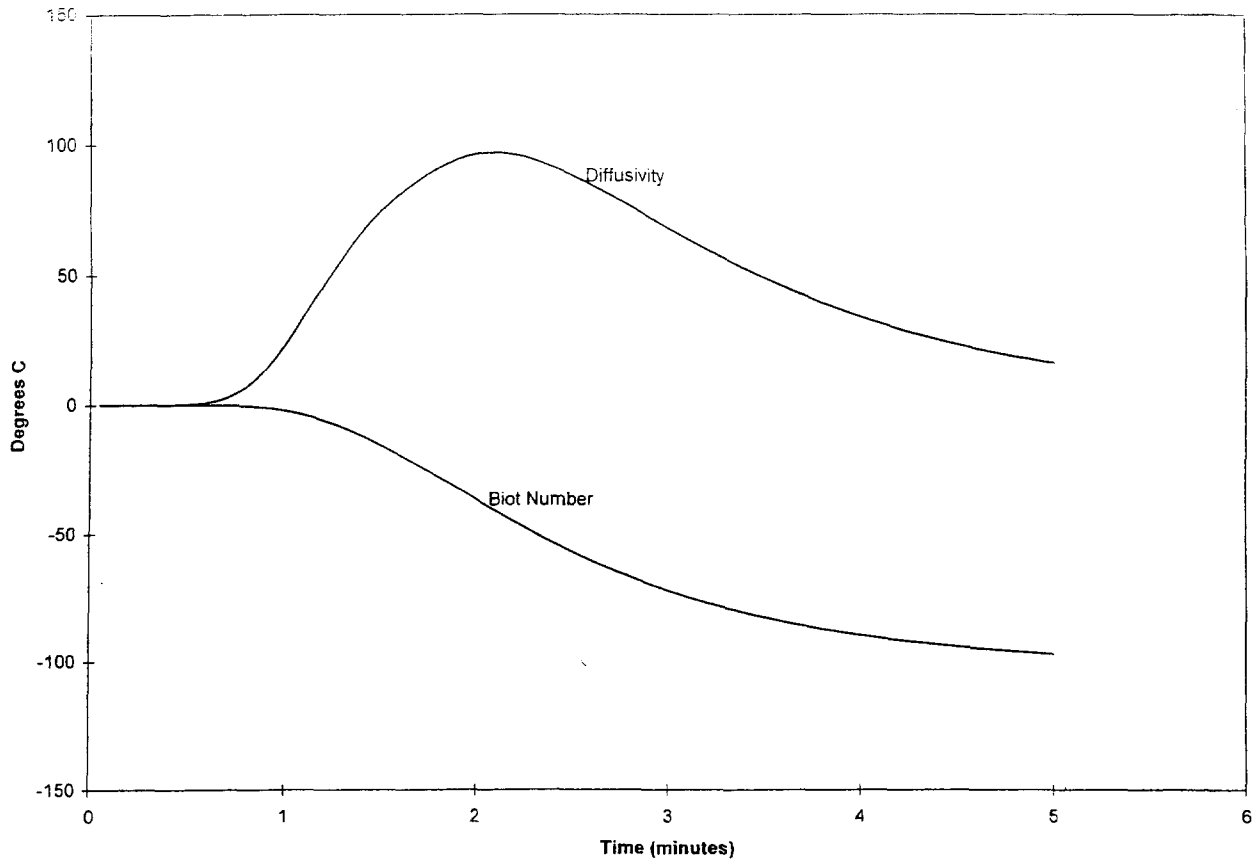
Figure 2 Sensitivity coefficients for the compound panel using the Direct Model of Section 2.1. The sensitivity coefficients are computed by finite differences, using the temperature solution at $x = L$, for test 2 data. Note that the functions are *linearly independent*. That is, a constant, whether positive or negative, multiplied by one function does not reproduce the other.

of the fiberglass compound material, the ΔT and Bi variations are lower.

The standard deviation of the residuals is a measure of the absolute variation discrepancy between the model predictions and the experimental data. A more accurate indicator of the agreement, however, is the ratio of the standard deviation of the residuals to the total temperature rise above ambient ΔT [1], sometimes called the "coefficient of variation." These values are presented in Table 1. For example, the standard deviation of the residuals for test 6 is smaller than for test 3 by a factor of 4. When comparing these quantities with respect to the ΔT during each test, however, the theoretical curve for test 3 is understood to be a more accurate model of the measurements than the same theory applied to test 6. The reason is that the chief means of comparison is the ratio of the standard deviation of the residuals to the total temperature change. In this example the ratio for test 3 is $8.59/336 = 0.0256$, which is smaller than the same ratio for test 6 given by $2.36/26 = 0.0908$. The latter ratio is bigger than the former by a factor of 5.

Figures 3 and 4 provide graphical plots of the residuals for tests 2–4 and 5–7, respectively. These graphs show that there is generally no systematic pattern in the residuals when comparing the experiments to one

another. There appears to be some correlation in the errors in the measurements for test 3, but the pattern is not repeated in the other tests. This correlation may be caused in part by the burn-off of the "scrim." In this test the thermal damage to the exposed face and underlying glass fiber was the most visually severe. One of the TCs was also noted to be in open air during part of the test (the data from this TC were not used). These data may manifest themselves in correlated errors when they are fitted into a theory based on Eqs. (2)–(4).

Figures 5 and 6 show plots of the two estimated parameters versus incident intensity. As a general trend, the estimated α is a monotonically increasing function of the incident intensity, whereas Bi exhibits an inverse relationship. For this plot, the intensity values were obtained by averaging the incident intensity over the first 5 min of the experiment.

Both behaviors can be explained by the appearance of the conductivity k in the numerator of α (which increases) and the denominator Bi (which decreases). This implies that the compound material conductivity increases with increasing temperature rise. The product α Bi $= hL/\rho c$, however, is not constant. This quantity changes as shown in Figure 7. If L and ρ are nearly constant during heating, and it is assumed that c is also
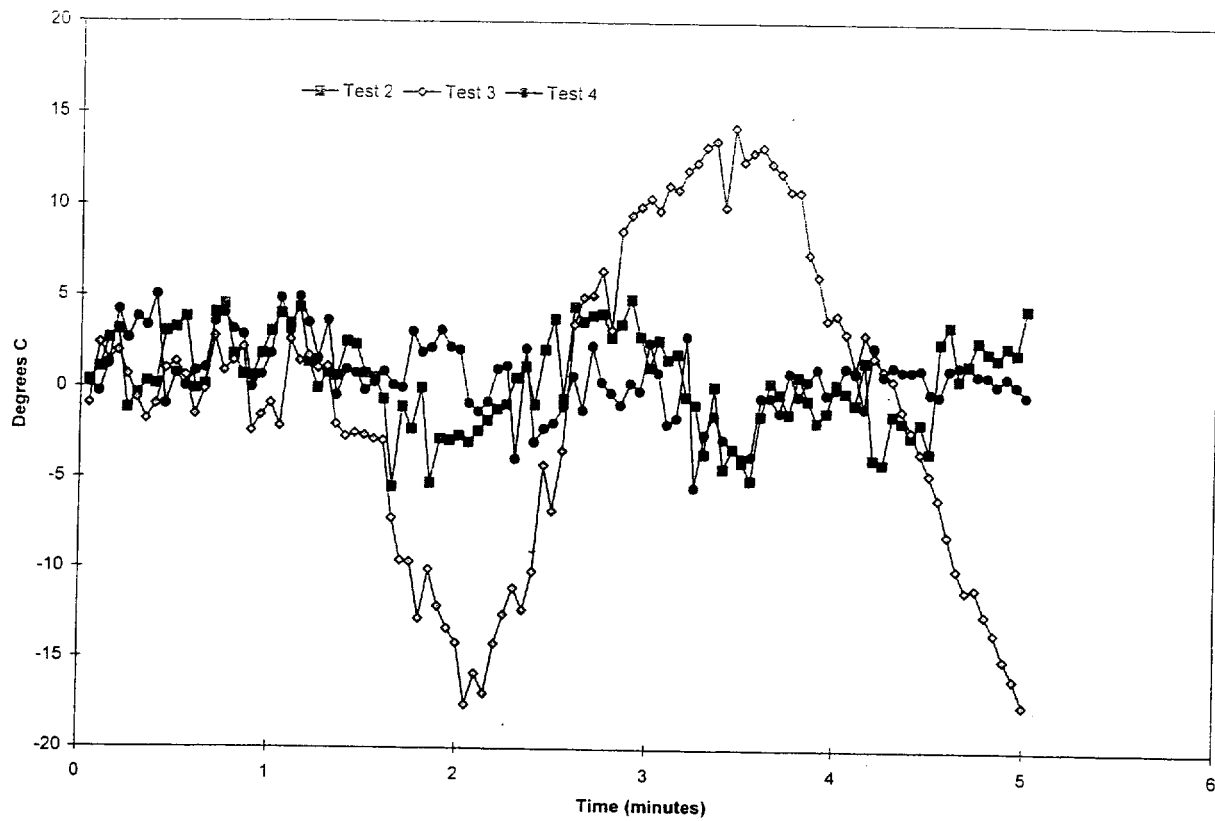
Figure 3 Residuals for tests 2–4. The lack of a systematic pattern between experiments indicates random errors rather than a misapplication of the model [1]. This suggests that the parameters derived are applicable to these tests in the manner that they were derived in Eqs. (2)–(4).
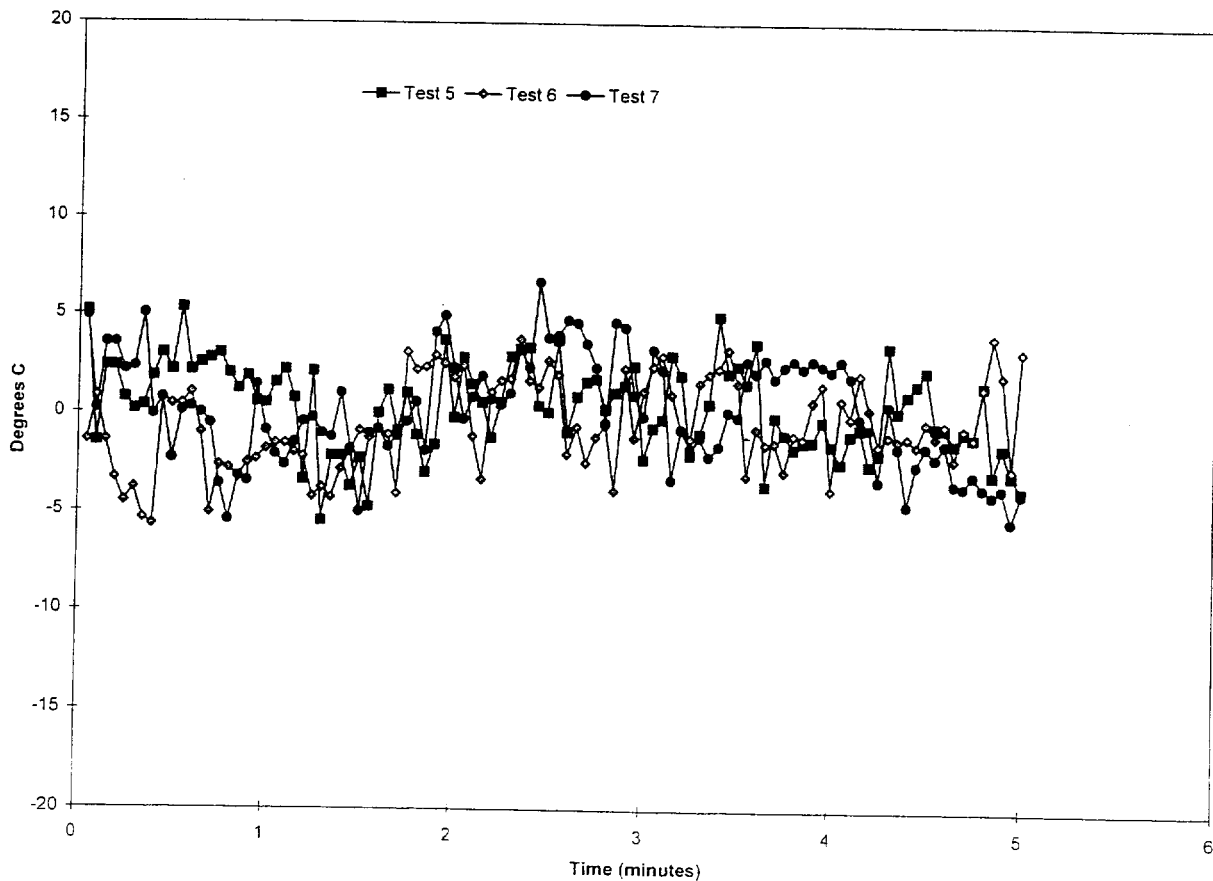
Figure 4 Residuals for tests 5–7. As with tests 2–4, there is no observable systematic error between experiments, indicating a reasonable fit [1] between the mathematical model and the experimental measurements.
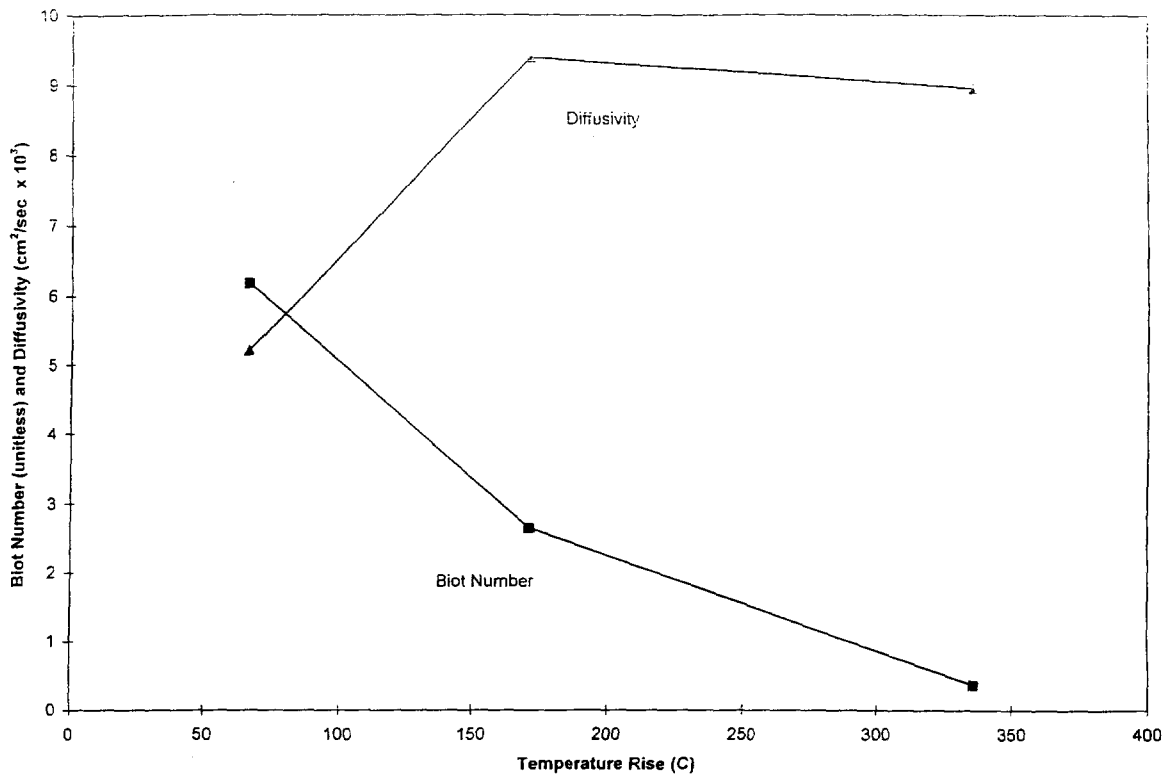
Figure 5 Plot of parameters versus temperature rise ΔT for tests 2–4. The diffusivity is generally monotonically increasing as a function of intensity whereas Biot number decreases monotonically. These changes suggest that the parameters are in fact functions of temperature because the temperature rise in the material is related to the incident radiant intensity (see Table 1).
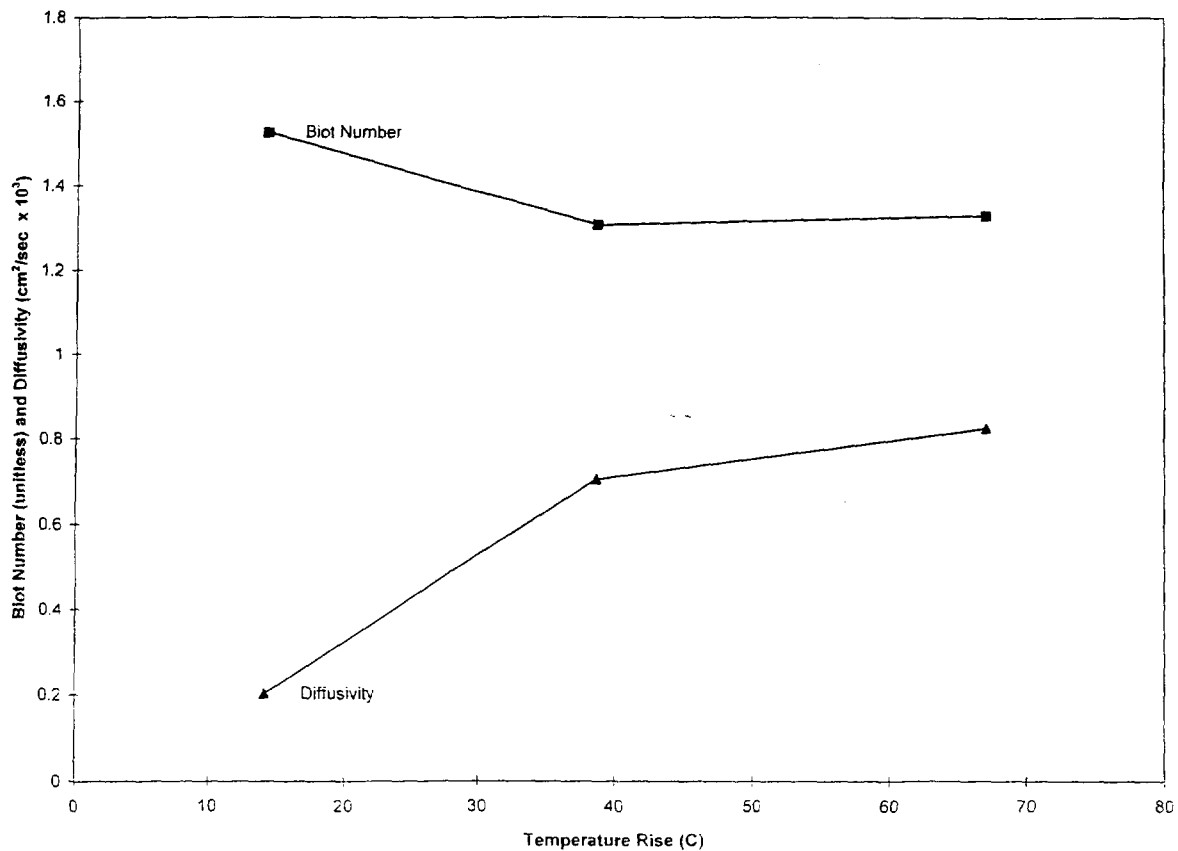
Figure 6 Plot of parameters versus temperature rise ΔT for tests 5–7. Although the material used in these tests has a much lower diffusivity, the trend for both parameters as functions of time is the same as in tests 2–4.
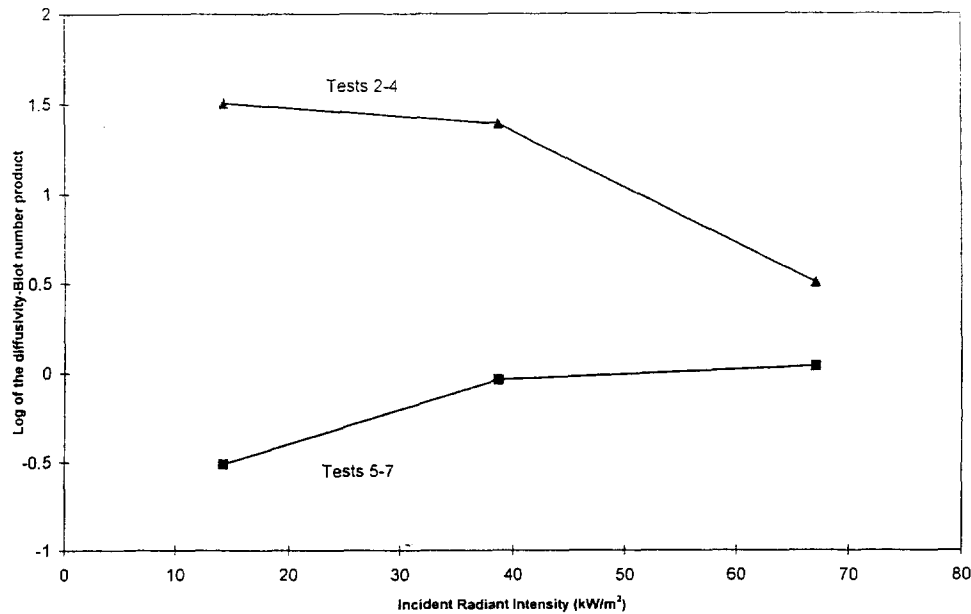
Figure 7 Plot of the logarithm of the product of α Bi as a function of incident intensity. This product essentially represents the heat transfer coefficient, assuming constant L, c, and ρ.

nearly constant, then these graphs represent the variation of h with temperature rise. As seen from Figure 7, the functional behavior of α Bi is opposite for the two materials: monotonically downward for tests 2–4 and monotonically upward for tests 5–7. An explanation of the behavior of Bi solely in terms of k is not sufficient. The explanation of α in terms of k is sufficient if the variation of ρc with T is much smaller. It is noted that, for all cases, temperature rise and heating intensity show qualitatively similar variations (see Table 1).

It is clear that Bi contains a "k part" and an "h part." The "k part" represents heat conduction through the compound material, whereas the "h part" represents convective heat transfer and radiant transfer to the ambient air behind the material. The latter can be changed independently of the material, for example, by blowing air with a fan across the back of the steel plate. In the experiments, there were no forced variations of h. An estimate of the dependence of h on temperature is obtained from the laminar free-convection Nusselt number correlation $\mathrm{Nu}_x = 0.59(\mathrm{Gr\,Pr})^{1/4}$ ($10^4 < \mathrm{Gr\,Pr} < 10^9$) as given in [13]. All properties are for the gas (air) rather than the solid plate. Using $\mathrm{Nu}_y = hy/k$, with y the local vertical position on the plate (see Figure 1), it is noted that, for constant k, $\mathrm{Nu}_1/\mathrm{Nu}_2 = h_1/h_2 = (\Delta T_1/\Delta T_2)^{1/4}$, where ΔT is the temperature difference between the plate and the ambient air. The numerical subscripts here denote the separate tests. It is assumed that negligible variations occur in Pr and β. If the latter variation is included, it can be shown instead that $h_1/h_2 = (\Delta T_1/\Delta T_2)^{1/4}(v_2/v_1)^{1/2}$ or $h_1/h_2 = (\Delta T_1/\Delta T_2)^{1/4}(T_2/T_1)^{3/4}$, since $v \approx T^{3/2}$ for diatomic gases [14]. Between tests 2 and 4, the ratio of heat transfer coefficients

is $h_2/h_4 = (171/66)^{1/4}(339/444)^{3/4} = 1.04$, between tests 6 and 5 the ratio is $h_6/h_5 = 0.87$, and between tests 6 and 7 the ratio is $h_6/h_7 = 1.19$. Using these relations yields $\mathrm{Bi}_i/\mathrm{Bi}_j = (h_i k_j/h_j k_i)$, which gives $\mathrm{Bi}_2/\mathrm{Bi}_4 = 0.43 = 1.04 k_4/k_2$, $\mathrm{Bi}_5/\mathrm{Bi}_6 = 0.86 = (1/0.87)k_6/k_5$, and $\mathrm{Bi}_7/\mathrm{Bi}_5 = 1.02 = (1.04)k_5/k_7$. These estimates give $k_4/k_2 = 0.4$, which implies that the compound conductivity between tests 2 and 4 decreases by 60% as ΔT diminishes from 171 to 66°C;. $k_6/k_5 = 0.75$, which indicates that a 25% decrease as ΔT diminishes from 68 to 26°C. Finally, $k_5/k_7 \approx 1.0$, yielding no change in compound conductivity even though the ΔT of the back face changes from 68 to 156°C.

These calculations suggest that the largest part of the Bi variation between tests is caused by the variation of k. From the k ratios and the α values of Table 1, it is possible to estimate the c ratios. Thus, $c_4/c_2 = 0.72$, $c_6/c_5 = 2.61$, and $c_5/c_7 = 1.17$. The data for tests 5–7 suggest that as ΔT increases, c decreases, since $c_5/c_6 = 0.383$ and $c_7/c_6 = 1.4$, and $\Delta T_2/\Delta T_4 = 171/66$.

3.2. Direct Model 2

The parameters estimated are shown in Tables 2 and 3. For these tests, data from the first 5 min of the experiment were used, which includes the transient portion of the experiment. The Biot number estimate uses the conductivity and thickness of steel, i.e., $L \approx L_S = 0.08$ cm, $k \approx k_S = 49.2$ W/m K in $\mathrm{Bi} = hL/k$. The heat transfer coefficient h, of course, is fixed for a given experiment and is independent of the assumptions made regarding the definition of the Biot number. For these

Table 2   Estimated parameters: insulation only, 300 s (Direct Model 2)

Test	Diffusivity (cm²/s)	Biot number (unitless)	Residual std. dev. (°C)	Temperature rise (°C)
2	0.009471	0.0075	2.737	171
3	0.00918	0.0011	7.784	336
4	0.00516	0.0096	2.145	66
5	0.000573	0.0026	2.227	68
6	0.000144	0.00075	2.420	26
7	0.000698	0.0032	2.702	156

Diffusivity estimates resemble those of Table 1, but the Biot number estimates differ by three orders of magnitude. This is due to the use of k_2 (thermal conductivity of steel) in the definition of the Biot number rather than conductivity of the overall compound material.

reasons, the Bi values computed here differ by approximately three orders of magnitude from those in Table 1. The wide range of temperatures makes suspect the assumption of constant parameters throughout the experiment. For this reason, it is advantageous to analyze separately the early portion of the experiment, which corresponds to a relatively small temperature rise. The assumption of constant properties is more appropriate over this shorter time interval (Table 3).

The advantage of analyzing this early portion of the experiment can be seen by examining the standard deviation σ of the residuals (the quantity σ is defined in the Nomenclature). The most drastic results are those of test 3. The residuals associated with this test are shown to develop a profound signature beyond 100 s in Figure 8. This signature in the residuals indicates a dis-

Table 3   Estimated parameters: insulation only, 100 s (Model 2)

Test	Diffusivity (cm²/s)	Biot number (unitless)	Residual std. dev. (°C)	Temperature rise (°C)
2	0.0116	0.018	1.916 (3.2%)	59
3	0.0107	0.013	1.683 (4.2%)	40
4	0.0325	0.45	1.820 (26%)	7
5	0.000467	0.019	2.327*	10
6	0.00953	0.15	3.053*	10
7	0.000593	0.0028	2.178	33

Same as Table 2 except the experiments were analyzed for only 100 s. The Bi values are still smaller than Table 1 but not as small as those in Table 2. This is due to the increased heat losses at the higher temperatures. *Required 180 s of data to converge.

parity between the experimental measurements and the mathematical model. Since this signature is present only in test 3, however, the disparity is thought to be caused by a failure in that particular experiment, such as a delamination of the insulation and the steel. As can be seen in Figures 3 and 4, there is no signature of any significance in the residuals from any of the experiments, with the exception of test 3.

The results for the analysis of the diffusivity of the insulation, for the case when the diffusivity of the steel was known, are consistent with the results for the diffusivity of the compound material when both materials were lumped together. Between Tables 2 and 3, the α values for tests 2–4 differ by about 1%, but those between tests 5–7 differ by 18–40%. The trends, however, are similar. The low conductivity and greater thickness of the insulating material, in comparison to the steel, dominates the numerical results. This means that there
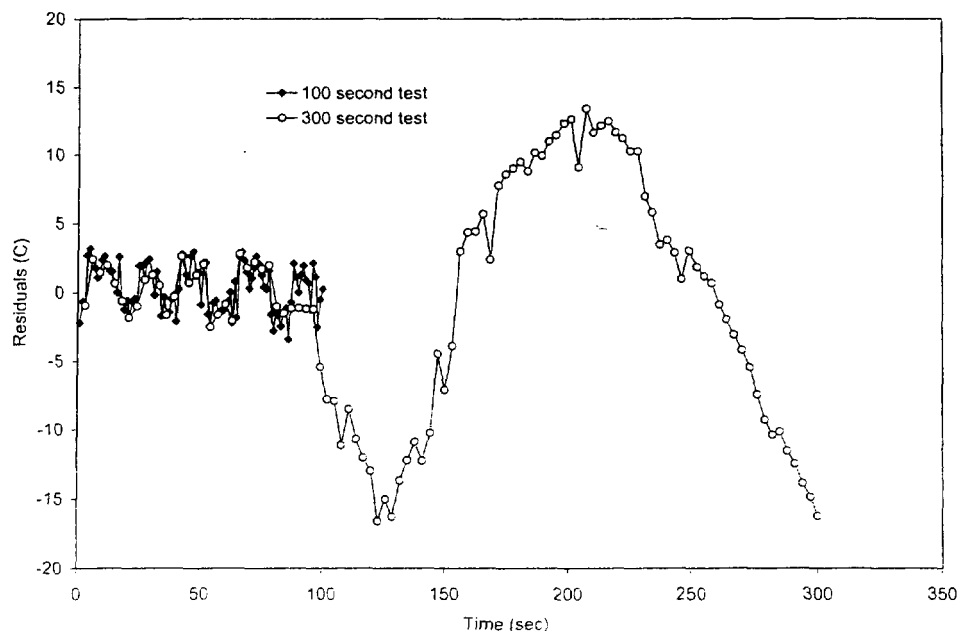

Figure 8   Residuals comparing 300-s interval to 100-s interval for test 2. Note that when the experimental data covering 300-s is analyzed, a distinct pattern becomes evident, indicating inadequate conformance of Direct Model 2 (300-s version) to measured data [1]. This is possibly caused by the variation of the material thermal properties during the course of the experiment.
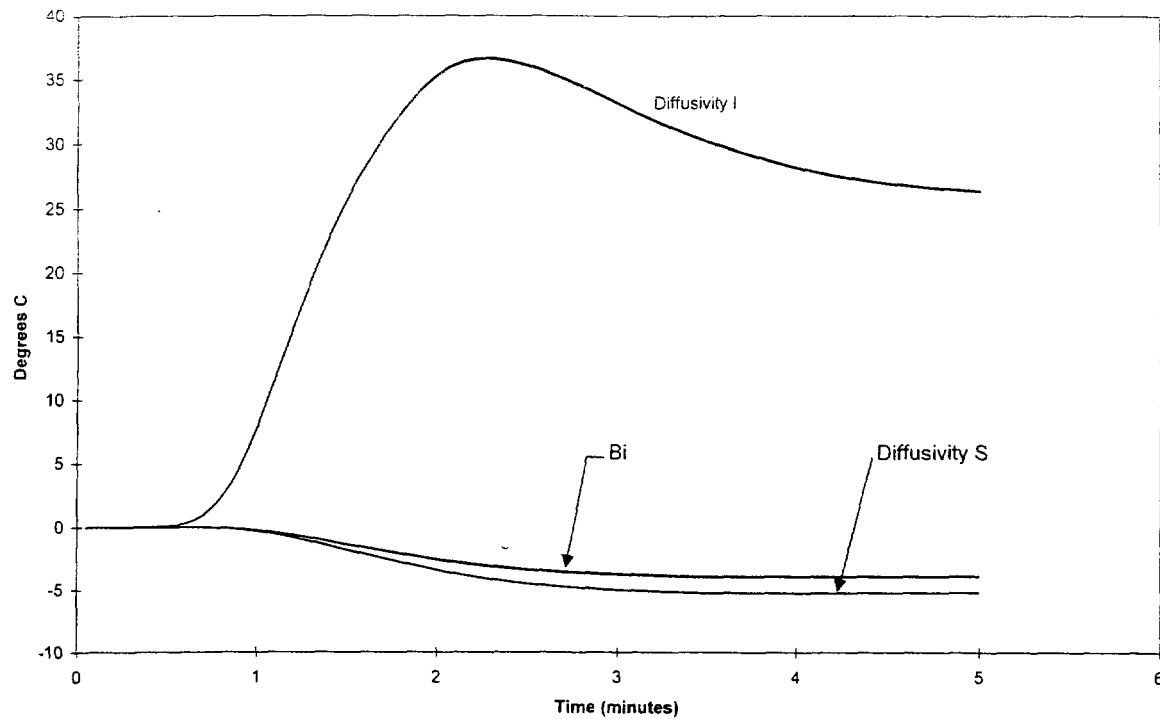
Figure 9 Sensitivity coefficients for the three-parameter case. The property labeled "Diffusivity I" pertains to the insulating material, whereas "Diffusivity S" is for the steel plate. Note the unacceptable correlation between Bi and Diffusivity S.

was little numerical difference in the results for tests 2–4, whether the insulation was considered separately or both materials were considered as one compound material. For tests 5–7 there were quantitative but not qualitative differences, and the orders of magnitude remained the same.

4. CONCLUSIONS

The least-squares method was used to estimate thermal parameters from data measured in radiant heating experiments using flat panels of various compositions exposed to different radiant heating intensities. The thermal parameters estimated from these measurements were α and Bi.

The results of the parameter estimation were produced by enforcing agreement between *measured back surface temperatures* and *computed back surface temperatures*. The estimated thermal parameter values varied between experiments because of the variation in measured temperatures. Other phenomena such as material breakdown and loss of contact between layers of the compound material may also have produced disagreement.

Models can be developed in which temperature variation of the thermal properties is accounted for, but these are much more complicated and consequently tend to be less robust. In addition, they involve estimation of more parameters, which is challenging. An

attempt was made to estimate *three parameters* simultaneously by solving the coupled energy equations in both insulation and steel panel. These three parameters were Bi, α_I, and α_S. When the sensitivity coefficients were plotted, however, a strong correlation was formed between Bi and α_S. For this reason, no subsequent parameter estimates were made using this model. Using the combination of model equations and experimental data, to estimate simultaneously four separate material properties for the insulation/steel plate assembly, parameter estimation results were not possible. Figure 9 shows the sensitivity coefficients for the three-parameter model. The correlation between Bi and α is obvious.

A detailed discussion of Bi was presented. The dependence of Bi on the combined insulation and steel thermal conductivity was described. In Section 3, the detailed T-dependence of Bi was examined. The behavior of Bi was in all cases consistent with physical predictions, except for test 3, as discussed. The results of the three models show identical trends, since the thermal diffusivity of the fiberglass insulation is approximately an order of magnitude larger than that of the aluminized silica.

The experimental apparatus used in the GM tests was not designed for thermal property parameter estimation. Nevertheless, in order to compute the heat transfer to and from assemblies such as those in Figure 1, estimates of compound material thermal properties are needed. This study has demonstrated that estimates of

such parameters can be made when the experiment is appropriately matched with the computation. The numerous scientific and engineering limitations of this type of modeling have been discussed.

A major question in this method of solution arises when one considers that the material layer is subjected to radiant fluxes at the front surface. If the radiant fluxes for the two materials (fiberglass, aluminized silica) are exactly identical, it is likely that the net heat flux passed into the materials differs because the material absorptivities and reflectivities differ. The glass fiber mat, which is black, absorbs more of the incident radiant flux than the reflecting aluminized silica cloth. This potentially difficult issue has been avoided by using only the *temperature data* at the front surface in the computations. That is, though the tests also measured the incident radiant flux, these data were not used because the reflected and absorbed portions could not be accounted for. If indepth absorption of the radiant flux is not known, accurately, the temperature of the front surface, as measured in the GM experiments, represents an accurate boundary condition for the heat conduction computation. Consequently, in principle (and subject only to the hypothesis that in-depth absorption of the radiant flux was negligible), the TC temperature measurements produce data that can be used reliably in the numerical simulations. Nevertheless, attaching and fixing the location of the TCs in the experiments was difficult: in response to the high incident fluxes, in one case (test 3) the "scrim" on the glass fiber mat burned off, rendering these data suspect. Given these qualifiers, the general order-of-magnitude agreement between test groups 2–4 and 5–7 is encouraging.

Research goals 2 and 3 identified in the introduction are now discussed (research goal 1 was discussed extensively throughout the article). For research goal 2 (the extent to which layered material can be considered as a single compound material) it was observed that the compound model (Model 1) generally functioned better than Models 2. Because of the applied-engineering nature of the experiments and the data gathered, the compound material approximation led to better results. Ideally, many more tests should be included in an analysis. For research goal 3 (why individual property models do not produce accurate predictions), it is noted that, though the two materials' properties may be known, a "third material" is created when the first two come into contact. This "material" is the boundary between the other two and, as has been discussed, its influence can be significant. It is also difficult to model and to understand. Discrete modeling in terms of the arrayed strands (for the fibrous material) holds promise. Studies using continuum ideas may proceed along ensemble averaging lines established in [8]. This is a major question that this research cannot possibly answer, but under whose influence many of the results were obtained and interpreted. The problem of heat transfer through finite-thickness fibrous materials near boundaries is one of ongoing significance.

NOMENCLATURE

Bi   Biot number ($= hL/k$)
c specific heat, J/m^3 K
g acceleration due to gravity, m/s^2
Gr   Grashof number ($= gx^3 \beta \Delta T / v^2$)
h heat transfer coefficient, W/m^2 K
k thermal conductivity, W/m K
L material thickness ($= L_1 + L_2$), m
N number of measurements
Nu   Nusselt number
p parameter value
Pr   Prandtl number ($= v/\alpha$)
q heat flux, W/m^2
S sum of squares of errors
t time, s
T temperature, K
T_∞ ambient temperature, K
T_j^i temperature calculated at $x = L$ at time step i at location j, K
x spatial dimension, m
X modified sensitivity coefficient, K
Y_i experimentally measured temperature measured at time step i, K
α thermal diffusivity ($= k/\rho c$), m^2/s
β coefficient of thermal expansion, K^{-1}
v kinematic viscosity, m^2/s
ρ density, kg/m^3
σ standard deviation of the measurement errors

$$\left[= \sqrt{(1/N) \sum_{i=1}^{N} (Y_i - T_i)^2} \right], \text{K}$$

Subscripts

i increment of time
l insulation
n parameter number
S steel
∞ surroundings

REFERENCES

[1] Beck, J., and Arnold, K., *Parameter Estimation*, Wiley, New York, 1987.
[2] Oladipo, A., and Wichman, I., Study of Thermal Barrier Materials Separating Automobile Engine and Passenger

Compartments. *Proc. 33rd ASME Natl. Heat Transfer Conf.*, Albuquerque, NM, August 15–17, 1999.

[3] Wichman, I., Beck, J., Oladipo, A., McMasters, R., and Little, E., Theoretical and Experimental Study of Thermal Barriers Separating Automobile Engine and Passenger Compartments, Final Report to GM Research and Development Center, Warren, MI, 2000.

[4] Relyea, H., White, M., McGrath, J., and Beck, J., Thermal Diffusivity Measurements of Free-Standing CVD Diamond Films Using Non-contacting, Non-destructive Techniques, *Diamond and Related Mater.*, vol. 7, no. 8, pp. 1207–1212, 1998.

[5] Bison, P., Muscio, A., and Grinzato, E., Thermal Parameters Estimation by Heating and Cooling and Thermographic Measurement, *Proc. SPIE—Int. Soc. Opt. Eng.*, vol. 3700, pp. 402–408, 1999.

[6] Dalbin, M., and Thomin, S., Method of Measurement of the Multilayer Woven Ceramic Matrix Composite Panel In-Plane Thermal Diffusivity, *J. Eur. Ceramic Soc.*, vol. 18, no. 1, pp. 59–63, 1998.

[7] Ozisik, M., *Heat Conduction*, 2d ed., Wiley, New York, 1993.

[8] Furmanski, P., and Floryan, J., Wall Effects in Heat Conduction through a Heterogeneous Material, *Int. J. Heat Mass Transfer*, vol. 37, no. 13, pp. 1945–1955, 1994.

[9] Santrock, J., Personal communication, 1997–1998.

[10] Forsyth, G., and Wasow, W., *Finite Difference Methods for Partial Differential Equations*, Wiley, New York, 1960.

[11] Haji-Sheikh, A., CONDS, Public-domain software available at www.BeckEng.com, 1991.

[12] Eshbach, O., *Handbook of Engineering Fundamentals*, Wiley, New York, 1963.

[13] Ozisik, M., *Basic Heat Transfer*, McGraw-Hill, New York, 1977.

[14] Vincenti, W., and Kruger, C., *Introduction to Physical Gas Dynamics*, Krieger, Melbourne, FL, 1986.

Robert L. McMasters IV is a Visiting Assistant Professor at Michigan State University in East Lansing, Michigan. He graduated from the U.S. Naval Academy, Annapolis, MD, in 1978 and subsequently served as a division officer on the *USS Will Rogers* (SSBN 659) and as an instructor at the S1W prototype. He has also served as a design engineer at K. I. Sawyer Air Force Base near Marquette, Michigan, and at Michigan State University. Since completing the Ph.D. in Mechanical Engineering, he has been conducting research in heat transfer and teaching classes in a wide range of mechanical engineering topics.

Indrek S. Wichman is a Professor of Mechanical Engineering at Michigan State University in East Lansing, Michigan. After obtaining his Ph.D. in 1983, he did a 2-year postdoctoral at NBS (now NIST), arriving at MSU in early 1986. His research interests may be accurately characterized as flame/surface interaction studies using analytical, numerical, and experimental techniques. Applications include flame spread over combustible fuels, ignition and quenching phenomena for gases, liquids, and solids, and fire research generally. He teaches courses in combustion, gas dynamics, micro-heat transfer/fluid mechanics, statistical thermodynamics, and classical thermodynamics.

56   heat transfer engineering   vol. 23 no. 4 2002